

RSRE MEMORANDUM No. 4258

AD-A205 380

REF FILE COPY

UNLIMITED

BR109030
②



RSRE
MEMORANDUM No. 4258

ROYAL SIGNALS & RADAR
ESTABLISHMENT

SPECTROSCOPIC ELLIPSOMETRY CHARACTERISATION OF
CVD DEPOSITION AND DOPING OF POLYSILICON
MULTILAYER STRUCTURES

Authors: S Sharma, C Pickering, A Morpeth, G R Terry

PROCUREMENT EXECUTIVE,
MINISTRY OF DEFENCE,
RSRE MALVERN,
WORCS.

DTIC
ELECTED
MAR 29 1989
S D
H

DISTRIBUTION STATEMENT A

Approved for public release;
Distribution Unlimited

UNLIMITED

89 3 28 051

0031532

CONDITIONS OF RELEASE

BR-109060

.....U

COPYRIGHT (c)
1988
CONTROLLER
HMSO LONDON

.....Y

Reports quoted are not necessarily available to members of the public or to commercial organisations.

ROYAL SIGNALS AND RADAR ESTABLISHMENT

Memorandum 4258

TITLE: SPECTROSCOPIC ELLIPSOMETRY CHARACTERISATION OF CVD DEPOSITION AND DOPING OF POLYSILICON MULTILAYER STRUCTURES

AUTHORS: S Sharma, C Pickering, A Morpeth, G R Terry

DATE: October 1988

SUMMARY

Polysilicon multilayer structures were prepared by a CVD process. Spectroscopic ellipsometry supported by a computer modelling facility was used to synthesise models of the polysilicon-on-oxidised-silicon multilayer structures. Deposition temperature, recrystallisation and doping were studied on both bulk and SOS silicon wafers. The accuracy of interferometry as a film thickness measurement technique on polysilicon was also assessed.

Copyright
C
Controller HMSO
London
1988

CONTENTS

	PAGE
1. INTRODUCTION	1
1.1 Object of Investigation	1
1.2 Description of Process	1
2. EXPERIMENTAL - MODELLING	2
3. RESULTS AND ANALYSIS	2
3.1 Oxidation	2
3.2 Poly Si Deposition at 580°C	3
3.3 580°C Deposition and Heat Treatment	4
3.4 Poly Si Deposition at 617°C	5
3.5 617°C Deposition and Heat Treatment	6
3.6 SOS Wafers and Thin Oxide Wafers	7
4. EVALUATION OF 'NANOSPEC' INTERFEROMETER MEASUREMENTS	8
5. SENSITIVITY AND ACCURACY OF FITS	9
5.1 Bulk B19	10
5.2 Bulk B15	10

Accession For	
NTIV GMA&I <input checked="" type="checkbox"/>	
DTIC X <input type="checkbox"/>	
Unpublished <input type="checkbox"/>	
JUL 19 1988	
FBI - BOSTON	
DEPT. OF JUSTICE	
(i) INVESTIGATORY CODE	
SEARCHED INDEXED SERIALIZED FILED	

5.3 Bulk B21	11
5.4 Bulk B17 and Bulk B23	11
5.5 SOS B5 and SOS B11	12
 6. OVERLAYER	
 7. EFFECT OF ANNEALING WITHOUT DOPANT	13
7.1 Annealing of 580°C As-deposited wafers	15
7.2 Annealing of 617°C As-deposited wafers	16
7.3 Discussion	17
 8. CONCLUSIONS	19
 20	

REFERENCES

APPENDIX 1: SENSITIVITY, MSE AND CONFIDENCE LIMITS

APPENDIX 2: IMPORTANCE OF OVERLAYER TO DEVICE FABRICATION

TABLE 1: CONSTITUENTS AND FILM THICKNESSES OF TREATED WAFERS

1A: BULK WAFERS

1B: SOS WAFERS

1C: THIN OXIDE WAFERS

TABLE 2: COMPARISON OF ELLIPSOMETRY AND NANOSPEC THICKNESS

READINGS

TABLE 3: CONSTITUENTS AND FILM THICKNESS OF UN-DOPED
ANNEALED WAFERS

1. INTRODUCTION

1.1 Object of Investigation

The purpose of this investigation was to use spectroscopic ellipsometry to non-destructively characterise a multilayer structure of polysilicon deposited on oxidised silicon wafers. The results gave information on the thicknesses of each individual layer and the fractions of the individual constituents which made up each layer.

The technique was used to determine the effect of temperature as a parameter in the deposition of polysilicon and to examine the effect of subsequent heat treatment to recrystallise the polysilicon. Further, the technique was used to assess the effect, if any, of the presence of dopant on recrystallisation. Multilayer structures as described above were produced on both bulk and silicon-on-sapphire (SOS) wafers. The technique is particularly important for measurement of SOS multilayer structures which are difficult to measure by familiar single wavelength techniques. These use a high (generally 633 nm) wavelength at which the light will penetrate through to the sapphire interface. A comparison was also made of spectroscopic ellipsometry vs. 'Nanospec' interferometry in determining the thickness of polysilicon.

1.2 Description of Process

Bulk Si wafers and SOS wafers, of epi-layer thickness 0.4 μm , were simultaneously furnace oxidised at 900°C to produce oxide thicknesses of 350 Å and 500 Å. Polysilicon was deposited at two temperatures; at 580°C to produce an amorphous layer and at 617°C to produce a layer with some crystalline (small grain) structure. Subsequently the wafers were doped and annealed in a POCl_3 furnace for 30 minutes at 900°C (followed by an HF etch to remove the resultant glassy overlayer). At each stage of the process, wafers were removed, and retained for spectroscopic ellipsometric examination.

2. EXPERIMENTAL - MODELLING

Measurements were made on a "SOPRA ES3G" rotating-polariser spectroscopic ellipsometer at an angle of incidence of 75° over a wavelength range 0.23 μm - 0.85 μm. The ellipsometer was controlled by a Hewlett-Packard HP300 series computer on which the relevant data parameters - cos delta and tan psi (the polarisation parameters, phase and amplitude ratio respectively of the light reflected from the sample surface) - were recorded as a function of the wavelength. The data were transferred to a "WYSE" computer with which the modelling was performed. It was attempted to synthesise a structural model which would give tan ψ and cos Δ values to match the measured data as closely as possible. The initial model was guessed intuitively, and parameters such as constituent fractions and layer thickness iterated by the computer, in an attempt to minimise the difference between data and model. The process was repeated until the closest possible match was obtained (with lowest mean square error - "MSE" - between the experimental data and the model). The effective dielectric function of individual layers were modelled by incorporating various constituents eg crystalline Si (Si), amorphous Si (α -Si), void, using the Bruggeman effective medium approximation¹.

3. RESULTS AND ANALYSIS

The results of the modelling performed on the measured wafers are displayed in Table 1. Underneath the designation is shown, in each case, the constituent elements of which each layer is composed and the layer thicknesses in angstroms. The treatments undergone by each wafer are indicated in the key.

3.1 Oxidation

The simplest treatment, namely oxidation, at 900°C causes the growth of, as seen in BULKB19, 489 Å of SiO₂. It was found that inclusion of a 6 Å interfacial layer of SiO

(modelled as 50% Si and 50% SiO_2) improved the fit. This layer could represent either the initial surface roughness of the silicon (the net effect upon oxidation being to produce a thin layer in which Si protrudes into the SiO_2), or possibly a non-stoichiometric sub-oxide SiO_x ($0 < x < 2$) at the interface. The equivalent SOS wafer (SOSB7) shows a thicker SiO layer probably indicating an initially rougher surface. This is in agreement with earlier work².

3.2 Poly Si Deposition at 580°C

For the as deposited 580°C polysilicon; reproduced below, Figure 1, it is seen that the polysilicon is largely amorphous with a small (2%) contribution from density deficits. The deficits could be missing atoms, vacancies, or microscopic volume deficiencies. These have been grouped together as "voids".

Figure 1. 580°C Polysilicon (as-deposited).

72% α - Si / 28% Void	-	23 Å
98% α - Si / 2% Void	-	3760 Å
SiO_2	-	497 Å
Si	-	Substrate

Also present is a thin, rough overlayer which is always associated with polysilicon deposition (see section 6). This overlayer will incorporate any native oxide present due to the similarity in dielectric functions of SiO_2 and voids. The amorphous nature of the deposited material is confirmed by the pseudo-dielectric function spectra, calculated assuming the wafer is a bulk sample, ie incorporating overlayers etc. In Figure 2, 580°C material is compared with standard amorphous silicon spectra³. No characteristic structural peaks are seen and the spectra are very similar to the amorphous case.

3.3 580°C Deposition and Heat Treatment

Having undergone the heat treatment it is seen, Figure 3, that most of the amorphous Si (94%) turns to crystalline grained material leaving a small amount of amorphous and void content probably associated with the grain boundaries. There is also a reduction, of around 7%, in polysilicon layer thickness due to consumption of Si to form a glassy overlayer removed by HF etching. In addition there is a three-fold increase in overlayer thickness probably due to grain structure formation upon heat treatment.

Figure 3a. 580°C Deposition and Heat Treatment.

76% Si / 13% α - Si / 11% Void - 90 Å
94% Si / 1% α - Si / 5% Void - 3541 Å
SiO₂ - 483 Å
Si - Substrate

Here the pseudo-dielectric spectra (Figure 3b) exhibit the familiar sharp characteristic maxima, at around 2950 Å, (and to a lesser extent at around 3650 Å) of crystalline silicon. It is compared with a computer generated amorphous spectra - clearly the sample has changed radically from amorphous silicon and is now very similar to the synthesised spectrum of crystalline silicon with a 25 Å SiO₂ overlayer. The loss of the peak structure near 0.36 μ m is due primarily to the effect of heavy doping and to a lesser extent to the microscopically rough surface overlayer. This is in agreement with other workers' findings³. The tan ψ , cos Δ spectra for this sample are plotted in Figure 3c. The equivalent sample on SOS is plotted in Figure 3d. Excellent agreement with the calculated curves can be seen, indicating that the layers are uniform with abrupt interfaces.

3.4 Polysilicon Deposition at 617°C

It is seen, in Figure 4, for the 617°C as-deposited case, that in addition to the rough overlayer the polysilicon was modelled as a two layer system as it was impossible to obtain an accurate model with a single polysilicon layer. Clearly it can be seen that, at this temperature, there is some crystalline structure; from TEM studies (Cullis et al, unpublished work) it is likely to be small grained. Of the two layers it is seen that the lower has the higher crystalline content. It is unlikely, that, in fact, two differentiable polysilicon layers exist. More likely, there exists a concentration gradient of the two constituents, Si and amorphous Si, which the computer program models with a discrete two layer system. This gradient may be due to the fact that the polysilicon which is approximated by the lower layer must have been exposed to heat much longer and so the grains have had more time to crystallise than the upper layer - hence the greater Si crystalline concentration in the lower layer.

Figure 4. 617°C Polysilicon (as deposited).

14% Si / 51% α - Si / 35% Void - 105 Å
20% Si / 58% α - Si / 22% Void - 1106 Å
94% Si / 2% α - Si / 4% Void - 3893 Å
SiO_2 - 497 Å
Si - Substrate

The amorphous content in the lower layer is likely to be associated primarily with the grain boundaries (due to its small volume fraction of 3%). In the upper layer the amorphous content (58%) dominates over the crystalline content (20%), indicating smaller grain sizes.

The overall structure of the film is compared, in pseudo-dielectric mode, to an ideal amorphous Si film in Figure 5. It is seen that there is a depressed central region ($0.3 \mu\text{m} - 0.4 \mu\text{m}$) indicating the presence of voids or roughness. Clearly, the graph is differentiable from purely amorphous Si and the structure in the polysilicon spectrum indicates some crystallinity. This spectrum is consistent with small grains as expected from the TEM results. Comparison of the 617°C as-deposited film with the 580°C as-deposited case reveals a substantial difference in the polysilicon thickness—in the 617°C case (4999 Å) compared with the 580°C case (3893 Å). This apparent increase in deposition rate may be due to the higher temperature easing the disassociation of the silane molecule in the pyrolysing process which creates polysilicon ($\text{SiH}_4 \rightarrow \text{Si} + 2\text{H}_2$) and/or an increase in the subsequent mass transport of Si to the oxide surface.

3.5 617°C Polysilicon Deposition and Heat Treatment

After the heat treatment it is seen, Figure 6, that the polysilicon layer shows an improvement in quality but only insofar as the upper layer becomes as 'good' as the lower one, ie the crystalline content of the upper layer increases to that of the lower layer. As a result the two previously distinct layers are no longer differentiable and there is just one layer whose overall quality is no better than that of the original (lower) layer. This is confirmed by a similar result on a SOS wafer which simultaneously underwent the same treatment.

Figure 6. 617°C Polysilicon Deposition and Heat Treatment.

61% Si / 10% α - Si / 28% Void - 75 Å
87% Si / 5% α - Si / 8% Void - 4787 Å
 SiO_2 - 505 Å
Si - Substrate

When comparing this result with the heat-treated 580°C case it is seen quite clearly that the 580°C sample is of a higher quality due to its greater crystalline content and its smaller amorphous and void content (which would affect conductivity). This agrees with previous work by Harbecke et al⁴. The following conclusions can therefore be drawn concerning the re-growth of polysilicon upon heat treatment (in the 617°C case): either the existing crystals act as seeds and expand, or new crystals grow around the existing ones or both these processes occur. In any case the final product (the polysilicon film) is apparently inferior to that obtained by the unconstrained growth of purely amorphous Si at 580°C. It should be noted that the presence of dopants will affect the crystallisation of polysilicon. Therefore it was thought useful to repeat the heat treatment only (without the addition of dopant) to assess its effect. This is described in section 7. Comparison of the heat treated 617°C case with its 580°C equivalent, on a pseudo-dielectric basis (Figure 6b) shows clearly the superiority of the 580°C case (upper spectrum). The effect is dominated by the overlayer as in the wavelength region of interest (up to 0.4 μm) the penetration depth is only 100–200 Å. The lowering of the epsilon (ϵ) magnitude, in the 617°C case, is due to density deficits – voids. Although the overall thickness of the overlayer is smaller, the percentage of voids is much higher so the total void 'volume' is greater and so the epsilon (ϵ) magnitude will be reduced.

3.6 SOS Wafers and Thin Oxide Wafers

The treatments described were carried out simultaneously on both Bulk and SOS wafers. It is seen, Table 1, that the constituent percentages and layer thicknesses were very close for all bulk and SOS wafers which underwent the same treatment. The use of a thinner oxide (350 Å) than 500 Å was investigated – BULKA21 and BULKB21 respectively. The magnitude of the differences in Poly-Si constituents between the two cases can be seen to be small. It can therefore be concluded that the oxide thickness reduction from 500 Å to 350 Å appears to have little or no effect on the polysilicon.

It was found that the Si epitaxial layer thicknesses on all the SOS wafers used were in a range within plus or minus 10% of each other - so satisfying the specification required of a batch. The "starting" thickness is unknown but upon oxidation about 3600Å of Si remains after the growth of 500Å of oxide. This suggests an initial pre-oxidation epitaxial layer thickness of around 3800Å.

4. EVALUATION OF "NANOSPEC" INTERFEROMETER THICKNESS MEASUREMENTS

The Nanospec instrument is a relatively simple interferometric tool used to measure silicon film thicknesses quickly. Its operation, based on an optical microscope, depends on finding, through interferometry of light from a film surface, an optical thickness for the film. The computer program that operates the instrument assumes a constant value for the refractive index (close to that of crystalline Si) and uses it to yield a value for the film thickness. Here the refractive index of polysilicon films is variable and differs from that of crystalline silicon so in this case the Nanospec may not be an accurate measurement tool. Table 2 lists the film thicknesses as measured by Nanospec interferometry on the bulk silicon wafers and by spectroscopic ellipsometry alongside the wafer treatments and the resultant layer constituents. It is seen that in some cases the Nanospec overestimates the thickness while in others it underestimates.

In the first case of 580°C polysilicon deposition, the film is virtually fully amorphous. The refractive index of amorphous Si is greater than that of crystalline Si in the region of Nanospec operation (0.39 μm - 0.8 μm). Therefore the instrument, having preset the refractive index too low, compensates by overestimating the film thickness (here by about 15%). In the second and fourth cases, heat-treated 580°C and heat-treated 617°C, voids are present in the film. This will act to reduce the overall refractive index so the Nanospec, having set the refractive index too high, will underestimate the thickness (by about 10% although the presence of 6% amorphous Si in the fourth case may complicate

matters somewhat by pushing the actual refractive index up). Finally in the third case, as-deposited 617°C polysilicon, it is seen that both amorphous Si and voids are present and the Nanospec underestimates the thickness: the effects of the voids appear to dominate. This is not surprising as there is a larger difference in refractive index between crystalline Si and voids (refractive index = 1) than between crystalline Si and amorphous Si.

To conclude then: the Nanospec works with greatest accuracy when measuring large-grain polycrystalline Si but it overestimates film thickness when amorphous Si is present and underestimates when voids are present.

5. SENSITIVITY AND ACCURACY OF FITS

In this section we examine the closeness of the fits of certain constituents to assess how sensitive the model is to them. (Appendix 1 discusses the relationship between sensitivity, mean-square error and confidence limits.) In order to validate comparisons between wafers all parameters were varied for every model. This has produced high correlation of some parameters, so not all parameters are at their optimum value. This is manifested in the sensitivity coefficients expressed as a relative change in the final MSE discussed below. In some cases a $\pm 1\%$ change in the parameter values causes a \pm change in the final MSE, instead of only positive changes which would be for optimum values. However the negative changes were small in magnitude indicating the results are close to optimum and little change in the best fit model was obtained by varying single parameters.

The 3-dimensional plot of Figure 7a shows the change in $\cos \Delta$ caused by a 50 Å change in buried SiO_2 layer thickness (from 350 Å to 400 Å) versus angle of incidence. The resulting sharp peaks are echoed in contour form in Figure 7b. The sample in question here is polysilicon on SiO_2 on SOS. The results show that greatest sensitivity occurs at angles of incidence near 75° and hence this angle has been used for all measurements.

5.1 Bulk B19

In this the simplest structure, SiO_2 is modelled onto SiO on a bulk Si substrate. The confidence limits on the SiO thickness are extremely wide (6.2 ± 4.8) Å and the change in Mean Square Error (MSE) associated with a 1% change in the modelled result is small ($0.18 \times 10^{-2} \pm 0.10 \times 10^{-3}$) indicating poor sensitivity to SiO thickness. In contrast the SiO_2 thickness is extremely well defined (488.6 ± 3.1) Å and the MSE change is very high ($0.18 \times 10^{-2} \pm 0.49$) indicating high sensitivity to SiO_2 thickness. The thinner oxide version of BULK B19 (BULK A19) has a nominal 350 Å oxide thickness (instead of 500 Å) and shows a similar, if less pronounced, effect namely that the sensitivity to SiO_2 thickness is greater than that to SiO thickness.

5.2 Bulk B15

This structure consists of deposited amorphous polysilicon (capped by a rough overlayer) deposited on SiO_2 grown onto a bulk Si substrate. The data indicates a very well defined polysilicon layer both in terms of constituency and thickness. The polysilicon layer amorphous percentage is (98 ± 3) and, predictably, there are large associated MSE changes of 1.6, for a -1% change in amorphous percentage, and 4.4 for a +1% change (the actual finishing MSE is 0.57×10^{-3}). An excellent (narrow) polysilicon thickness confidence limit is also obtained (3759.7 ± 34.3) Å along with very high MSE changes of 4.4 and 10.3. Polysilicon thickness and amorphous concentration appear to be highly correlated (0.991 compared with a theoretical maximum of 1.0) so the program appears to have successfully balanced the effect of two highly sensitive parameters.

Elsewhere, the model exhibits poor overlayer confidence limits (23.3 ± 8.9) Å. These loose confidence limits are associated with relatively small MSE changes of 0.14 and 0.16×10^{-1} (compared with the polysilicon described above) indicating poorer sensitivity.

Insofar as the overlayer thickness itself is small the limits cannot be expected to be well defined although the amorphous percentage within the overlayer has tightly defined limits (72.2 ± 0.1). In addition there is a high degree of correlation between polysilicon thickness and overlayer thickness so the high sensitivity to the former allows the determination of optimum values. Finally for the (buried) SiO_2 thickness although the confidence limits are well defined (496.5 ± 18.8) Å the MSE changes are small (-0.7×10^{-2} and 0.16×10^{-1}) indicating poor sensitivity. In conclusion then the sensitivity is highest for polysilicon thickness, it is lower for overlayer thickness and worst for SiO_2 thickness.

5.3 Bulk B21

This sample is modelled in 5 layers - a rough overlayer capping an upper and a lower polysilicon layer deposited on a thermally grown SiO_2 layer on bulk silicon. Because this is only a very approximate representation of a probably continuously-varying grain size profile the fitted parameters are only indications. The sensitivities for this sample will not therefore be discussed in detail.

5.4 Bulk B17 and Bulk B23

These samples have similar structures - a rough overlayer capping a (doped and annealed) polysilicon layer, above a thermal oxide, on a bulk Si substrate. The difference between them is that polysilicon deposition was at 580°C for Bulk B17 and at 617°C for Bulk B23. Both these samples exhibit similar trends in sensitivity and fit accuracy as enumerated below.

1. The polysilicon layer exhibits very high sensitivity - the MSE changes (-1% and 1%) are (for Bulk B17 and Bulk B23 respectively) 13.9 and 13.8, 11.3 and 10.6 cf finishing MSE's of (0.93×10^{-3} ; 0.36×10^{-2}).

2. There is a correspondingly very tight confidence limit specification on polysilicon thickness - (3541 ± 44) Å for Bulk B17 and (4787 ± 61) Å for Bulk B23.
3. A high degree of correlation exists between the inter-polysilicon crystalline and amorphous concentrations but this is balanced by high sensitivities for crystalline silicon (-1% and 1% changes of 6.5 and 5.6 for Bulk B17 and 7.8 and 4.5 for Bulk B23). As expected with such high sensitivities the associated confidence limits are very tight (94 ± 5) % for Bulk B17 polysilicon crystalline content and (87 ± 3) % for the corresponding element in Bulk B23.
4. The SiO_2 exhibits a far superior confidence limit specification of (for Bulk B17 and Bulk B23 respectively) (483 ± 14) Å and (505 ± 27) Å compared with overlayer fit of (90 ± 26) Å and (75 ± 20) Å. The sensitivity ($\pm 1\%$ changes) of overlayer and SiO_2 thickness are however of the same order of magnitude.

5.5 SOS B5 and SOS B11

The above samples are chosen to illustrate the effects of modelling on SOS substrates. Their direct bulk equivalents are Bulk B17 and Bulk B23.

The principal feature to emerge from their models is that there is an astonishingly well defined confidence limit specification for the epitaxial silicon layer - (3611 ± 3) Å and (3622 ± 2) Å for SOS B5 and SOS B11 respectively. This could be due to the fact that the change in thickness of the Si layer tends to cause a lateral shift in peaks in the $\cos \Delta$ and $\tan \psi$ spectrum, particularly in the high wavelength region, resulting in large MSE differences for relatively small thickness variations. Other manifestations of parameter fluctuation (peak height change, peak broadening, increase in $\cos \Delta$, $\tan \psi$ at low λ 's, etc) cause smaller MSE changes to take place. A high sensitivity (MSE variation) would be

expected for this layer - however this is not the case, $\pm 1\%$ changes for eg SOS B11 are 4.96 and 2.60 compared with 8.25 and 9.01 for the polysilicon layer. However the confidence limits of the polysilicon thickness will be increased due to incorporation of variable percentages of other constituents, causing correlation problems.

The sensitivity of the polysilicon layer compared to the equivalent bulk cases, is slightly reduced and this manifests itself in slightly inferior confidence limits (eg SOS B5 has a polysilicon layer sensitivity ($\pm 1\%$) of 4.2 and 2.1 whereas its bulk equivalent (Bulk B17) has sensitivities of 13.9 and 13.8. The resulting confidence limits are reduced from (3541 ± 44) Å to (3483 ± 80) Å. A similar effect is echoed in the overlayer.

So to conclude, on SOS the epitaxial silicon layer is fitted to a high degree of confidence. Elsewhere the polysilicon fit and sensitivity are eroded somewhat by the "inclusion" of an SOS substrate but the patterns of sensitivity and fit quality, described for the bulk cases, remain the same for polysilicon, SiO_2 and overlayer.

6. OVERLAYER

As discussed before there is a rough overlayer associated with polysilicon deposition. Its origin may be attributed to two sources: the first is that as the top surface of the as-deposited polysilicon is readily susceptible to oxidation then if many different oxidation planes are exposed, each with its own characteristic oxidation rate, then they will produce, microscopically, a rough surface. So Bulk B15 and Bulk B21 must exhibit an overlayer as they both have as-deposited polysilicon layers. Amorphous Bulk B15 has 23Å of overlayer which is mainly native oxide since no well defined planes exist. The relationship the overlayer shares with the underlying polysilicon layer is that it possesses a smaller crystalline silicon concentration, a smaller amorphous silicon concentration and a compensatory larger void concentration. Although SiO_2 might be expected in the overlayer, this is not seen in the models. In fact any SiO_2 present in the overlayer

would probably be represented, at least in part, by the voids due to the similarity in dielectric functions.

Another interesting feature to note is that the 617°C as-deposited case (Bulk B21) has a threefold thicker overlayer than the 580°C case (90 Å vs 23 Å). This may be because in the 617°C case, the existence of a few grains imposes a non-random orientation of growth planes on the surface, some of which may be much more susceptible to developing roughness - hence microscopically the surface could be rougher than a completely random, unordered, amorphous structure. In addition, as was noted earlier, the 617°C case exhibits (possibly) a graded polysilicon bulk which the model attempts to simulate as discrete layers - perhaps some of the underlying polysilicon layer is in fact incorporated in the overlayer. Direct comparisons between overlayers would, were this true, be invalid.

The second reason for overlayer formation is because POCl_3 doping is performed in an oxygen ambient at 900°C. The POCl_3 breaks up with phosphorus diffusing into the polysilicon via the grain boundaries and a phosphorus-doped silicon dioxide (p-glass) overlayer is formed. To make an insulator above the polysilicon (of controllable thickness) the p-glass is removed by a sixty-second HF etch and an LTO (low-temperature-oxide) is deposited. During the HF etch it is possible that preferential etching takes place - so some planes will be etched more than others resulting in a microscopically rough overlayer.

After the heat treatment the overlayer, as expected, improves in quality but an interesting phenomenon takes place with regard to its relationship with the underlying polysilicon layer. Whereas in the as-deposited case the amorphous silicon content in the overlayer is less than that in the polysilicon, here it is greater (the void concentration is, as before, greater). This may be due to the annealing process which will recrystallise from the oxide - amorphous interface upwards tending to push unstructured regions upwards towards the overlayer.

7. EFFECT OF ANNEALING WITHOUT DOPANT

In this section it was sought to establish the role of the dopant - Phosphorus - in the recrystallisation process. This was done by allowing as-deposited samples to undergo POCl_3 -like thermal-cycles in the absence of POCl_3 . It is necessary to clarify the impurity doping effect on recrystallisation because the low resistivity requirements of polysilicon gates require heavy doping which is thought to increase polysilicon grain size and so degrade delineation⁵. This could lead to a variation in gate length - of particular important in sub-micron regimes.

Initially it was proposed to simulate the POCl_3 heat cycle - loading (and unloading) samples in N_2 sandwiching a 35 minute N_2/O_2 mixture (ratio 95%:5%) exposure at 900°C. However, this takes no account of the formation of a glassy - "P-Glass" - phosphorus-doped oxide overlayer during the POCl_3 doping process. Such a layer would be formed at the elevated doping temperature (900°C) when the POCl_3 molecule dissociates. The dopant P diffuses into the polysilicon (mainly via the grain boundaries) and the oxygen forms (a phosphorus-doped) SiO_2 layer. (The Cl_2 molecule will be removed as a by-product, probably HCl).

The formation of the glassy layer itself influences the recrystallisation in three ways:

- i. The physical presence of an oxide overlayer above the polysilicon will affect the heat flow to and therefore the temperature of the polysilicon.
- ii. The growing oxide whose interface advances into the polysilicon will cause a redistribution of the doping profile (ie segregation coefficient) of phosphorus entering the polysilicon. Therefore the oxide layer affects the concentration of dopant entering the polysilicon and so affects the structure of the recrystallising polysilicon. To influence the

polysilicon structure appreciably the oxide must substantially reduce the diffusivity of phosphorus impurities passing through it. This is because the high diffusivity of phosphorus in polysilicon results in the dopant rapidly reaching the solid solubility limit. Therefore to effect any change on the recrystallisation the oxide must slow down or prevent the attainment of this limit.

iii. The oxidation process itself may alter the random orientation of grains in the overlayer and so may affect its regrowth.

Therefore the as-deposited polysilicon wafers were cleaved in half and underwent heat treatment (at 900°C for 35 minutes). One half was heated in a nitrogen environment to test the effect of annealing without doping and the other half in an oxygen environment to find out if a capping layer (here undoped SiO₂) influences the recrystallisation.

7.1 Annealing of 580°C As-Deposited Wafers

Table 3A shows the fitted models for the 580°C as-deposited polysilicon samples after annealing in nitrogen, BULKB14N, and in oxygen, BULKB14O. It is seen that the structures are essentially similar save for the thick, 1066Å, SiO₂ overlayer on BULKB14O. The presence of this overlayer can be used to explain the two other major differences between the models namely the difference in polysilicon layer thickness and the presence of a thin, rough, polysilicon overlayer on the nitrogen-ambient-treated sample but not the other one. The polysilicon thickness is reduced in the oxygen-treated case due to the growth of SiO₂ which consumes polysilicon. The lack of a polysilicon overlayer in the oxygen-treated case can be attributed to the difficulty in modelling the data, Figure 8, in which the oxide layer manifests itself as a sharp, high magnitude peak in the tan δ spectrum. Accurate modelling of this peak necessitates a loss of accuracy in modelling adjacent smaller peaks. Further the overlayer in BULKB14N is very similar in composition (albeit with extra amorphous content) to its underlying polysilicon. In

BULKB14O such an overlayer would tend to be incorporated in the polysilicon layer. Indeed this may have taken place - the polysilicon layer in BULKB14O has a slightly higher amorphous content than BULKB14N.

Oxide Removal

The oxide overlayer in BULKB14O was removed in a 60 second NH₄F:HF (= 5:1 solution) etch. The result - B14O was plotted (in pseudo-dielectric form) in Figure 9 alongside the 580°C as-deposited sample, BULKB15 and the POCl₃-doped sample, BULKB17.

Four conclusions can be drawn from this plot:

- i. The characteristic peaks, in the imaginary spectrum at around $\lambda = 0.295 \mu\text{m}$ and $\lambda = 0.36 \mu\text{m}$ demonstrates the sample's essentially crystalline nature. (The closeness of the P-doped sample to crystalline silicon, capped by a thin oxide layer, has already been shown in Figure 3b.)
- ii. Recognising that dielectric function is equivalent to polarisability per unit volume then the slightly reduced overall amplitude of the P-doped spectrum BULKB17, compared to the undoped spectrum B14O, shows it contains more density defects (voids). Indeed the models show 5% voids for BULKB17 and zero per cent voids for B14O.
- iii. The reduction in magnitude, in BULKB17, of the $\lambda = 0.36 \mu\text{m}$ peak compared to the $\lambda = 0.295 \mu\text{m}$ peak is due to heavy P-doping as observed previously by Aspnes and Studna³.
- iv. Finally, it can be concluded that the presence of POCl₃ in the heat cycle has little effect on the recrystallisation of amorphously-deposited material.

7.2 Annealing of 617°C As-Deposited Wafers

It was attempted to model the 617°C as-deposited wafers with the capping oxide intact as in the 580°C case. However the complexity of the polysilicon layers made achieving a satisfactory model unachievable. Therefore the oxide overlayers were removed in a 5:1 buffered HF etch. It was demonstrated, the 580°C case, that this etch stopped within ~2 monolayers of the oxide-polysilicon overlayer interface ie that it did not remove any polysilicon.

Table 3B shows the resulting models of nitrogen and oxygen-ambient annealed wafers. It is seen that layer constituents in B20O and B20N are very similar the major differences arising in layer thicknesses. The oxygen-ambient case, B20O, has a thinner lowermost polysilicon layer with the result that the layers sandwiching it are thicker than in the nitrogen-ambient case. In the oxygen-ambient case the growth of a thick oxide cap reduces heat flow to and therefore crystallisation of the lower region of the polysilicon. This goes some way towards explaining the reduced thickness of the lower polysilicon layer in B20O but the cause of the greatly increased SiO₂ thickness - 574 Å is unknown. The 2-layer nature (ie graded grain size) of the as-deposited polysilicon has remained after the heat treatment in this case, whereas in the presence of P a uniform layer was obtained.

The pseudo-dielectric spectra of the oxygen-ambient sample, the as-deposited sample (BULKB21) and the POCl₃ doped sample (BULKB23) are plotted in Figure 10. Clearly it is seen that, unlike the 580°C case discussed in section 7.1, the inclusion of POCl₃ in the heat cycle produces an improvement in crystalline quality. The modelled structures of B20O (Table 3) and BULKB23 (Table 1A) confirm this.

7.3 Discussion

Comparison of Figures 9 and 10 show that phosphorus doping aids the recrystallisation of polysilicon deposited at 617°C. Nevertheless the quality of annealed polysilicon deposited at 580°C remains superior to that of annealed polysilicon deposited at 617°C.

To explain how P-doping aids recrystallisation the crystallisation mechanism is discussed. The fundamental grain growth process - by grain boundary migration - is believed to be a diffusion-controlled mechanism - ie by a series of diffusion jumps of individual Si atoms across grain boundaries. The growth rate is determined by the rate of diffusion of atoms across each grain boundary. The nett effect is to favour the growth of some grains at the expense of others.

The presence of phosphorus plays two roles: to increase the vacancy concentration (by shifting the Fermi level) and to enhance the grain-boundary mobility. The mobility determines the atom migration rate by the expression⁶

$$\mu = \frac{Dg}{kT}$$

where μ = mobility

k = Boltzmann's constant

T = Temperature

and Dg = Grain boundary diffusion coefficient.

Assuming single boundary migration, Dg can be replaced by D^b - the grain boundary silicon self-diffusion coefficient across the boundary. It is D^b which is enhanced by P-doping.

Such grain-growth enhancement can occur at 617°C because there are already small grains in existence amongst which Si atom diffusion can take place. At 580°C, however, there

are no grains present in the as-deposited sample so the first stage of recrystallisation - namely clustering of Si atoms to form small grains - must take place. In this situation unconstrained grain growth can occur with or without the presence of P.

In Figure 9 (the 580°C case) the lack of a rough overlayer on the undoped annealed sample, B14O, (the doped sample BULKB17 has a 90 Å thick layer) could contribute partly to its apparent superiority.

8. CONCLUSIONS

Spectroscopic ellipsometry has been used to successfully model the multilayer structure - polysilicon on oxide on silicon (both bulk and SOS) at two CVD deposition temperatures, 580°C and 617°C.

It has been shown that polysilicon deposition is largely amorphous at 580°C and small-grained crystalline at 617°C.

Upon recrystallisation it has been shown that the low temperature case produced a higher quality polysilicon layer than the high temperature case. The recrystallised low temperature case remained superior regardless of whether or not dopant was employed, although doping in a phosphorus (POCl_3) environment improves polysilicon layer quality deposited at 617°C case.

Finally, interferometric thickness measurement accuracy was shown to be dependent on the closeness of the polysilicon film to single-crystal silicon.

REFERENCES

1. D E Aspnes, J B Theeten*, Phys Rev B, Vol 20, 8, 3293 (1979).
2. C Pickering, S Sharma, Journal de Physique, C4-55 (1988).
3. D E Aspnes, A A Studna, Phys Rev B, Vol 29, 2, 768 (1984).
4. G Harbeke, L Krausbauer, Appl Phys Let, 42 (3), 249 (1983).
5. Y Wada, S Nishimatsu*, J Electrochem Soc, 125(A), 1499 (1978).
6. L Mei, M Rivier, J Electrochem Soc, 129(8), 1791 (1982).

APPENDIX 1: SENSITIVITY, MEAN SQUARE ERROR AND CONFIDENCE LIMITS

If a quantity has tight confidence limits associated with it then a calculated value of the quantity, must fall very close to the actual value. If however the quantity has wide confidence limits the calculated value may not be so close to the real value. Suppose there is a measure of the proximity of a modelled result to the actual quantity - the Mean Square Error (in fact the MSE is a measure of the difference between the measured graph and the modelled graph). If a 1% change occurs in the value of a fitted parameter and it causes a large change in the associated MSE then the sensitivity to that measurement must be great. Also if the confidence limits are very tight, the value of the quantity must be very accurately known - so small deviations from it will cause large changes in MSE. Therefore in conclusion, in general, tight confidence limits are associated with high sensitivity and large resultant MSE changes for a 1% change in the estimate of a quantity.

APPENDIX 2: IMPORTANCE OF OVERLAYER TO DEVICE FABRICATION

As far as achieving the low resistivity necessary for gate contacts for devices the presence of an overlayer as long as it is thin, as it is here, is unlikely to be significant. This is because the polysilicon, even though it is n-doped, would be saturated by phosphorous so leading to a high surface concentration of dopant and the resultant band bending would cause a high concentration of carriers in a very thin accumulation region so tunneling would occur. A 'good' contact between gate metal and polysilicon is thus assured. To assess the effect of the overlayer on device quality polysilicon samples of decreasing thickness would need to be produced to establish whether or not the overlayer is significant. However overlayer thickness may decrease with polysilicon thickness reducing the validity of such an experiment.

TABLE 1. Constituents and Thicknesses of Treated Wafers.

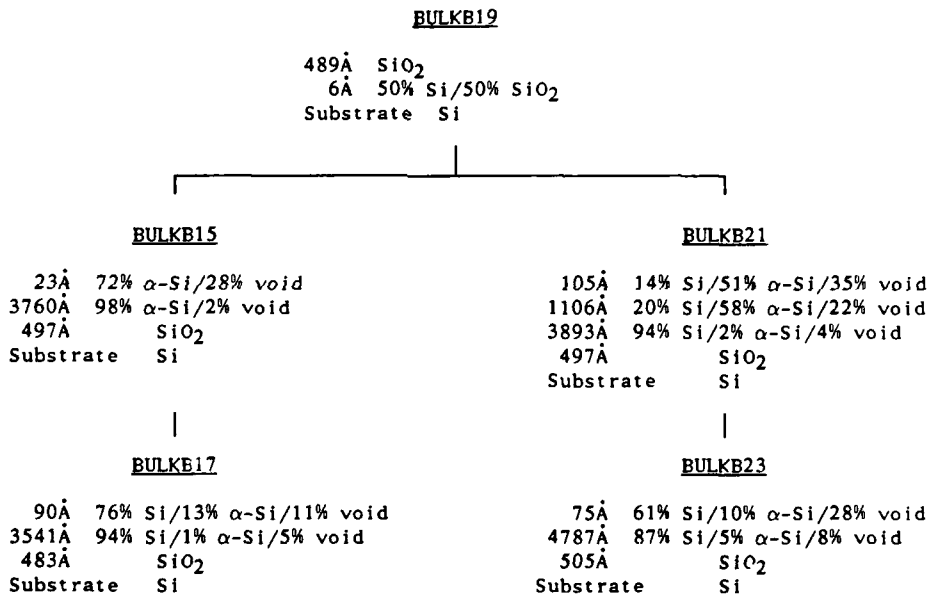
Key to Treatments:

OXIDE
DEPOSITION

580°C polysilicon deposition 617°C polysilicon deposition

Doping & Annealing Doping & Annealing

1A: RESULTS FOR BULK WAFERS



1B: RESULTS FOR SOS WAFERS

<u>SOSB7</u>	
493Å SiO ₂	
14Å 50% Si/50% SiO ₂	
3970Å Si	
Substrate Al ₂ O ₃	
<u>SOSB3</u>	
23Å 75% α-Si/25% void	
3775Å 97% α-Si/3% void	
499Å SiO ₂	
3781Å Si	
Substrate Al ₂ O ₃	
<u>SOSB9</u>	
104Å 13% Si/54% α-Si/33% void	
1172Å 18% Si/59% α-Si/23% void	
4040Å 85% Si/1% α-Si/14% void	
487Å SiO ₂	
3632Å Si	
Substrate Al ₂ O ₃	
<u>SOSB5</u>	
89Å 73% Si/10% α-Si/17% void	
3483Å 93% Si/3% α-Si/4% void	
503Å SiO ₂	
3611Å Si	
Substrate Al ₂ O ₃	
<u>SOSB11</u>	
63Å 62% Si/10% α-Si/28% void	
4901Å 86% Si/3% α-Si/11% void	
502Å SiO ₂	
3622Å Si	
Substrate Al ₂ O ₃	

1C: RESULTS FOR THIN OXIDE VERSIONS (OF BULKB19, BULKB21, SOSB5
RESPECTIVELY)

BULKB19

352Å SiO₂
10Å 50% Si/50% SiO₂
Substrate Si

BULKB21

100Å 14% Si/52% α-Si/32% void
987Å 20% Si/61% α-Si/19% void
4099Å 87% Si/2% α-Si/11% void
426Å SiO₂
Substrate Si

SOSB5

82Å 72% Si/10% α-Si/18% void
3378Å 97% Si/2% α-Si/1% void
352Å SiO₂
3699Å Si
Substrate Al₂O₃

TABLE 2. Comparison of Ellipsometry and Nanospec Thickness Readings.

WAFER TREATMENT	CONSTITUENTS (%)	SE (Angstroms)	NANOSPEC (Angstroms)
580°C POLYSILICON DEPOSITION	98% α-Si 2% void	3760	4300
580°C POLYSILICON DEPOSITION	94% Si 1% α-Si 5% void	3540	3302
+ DOPED & ANNEALED			
617°C POLYSILICON	20%Si/58%α-Si/22%void 94%Si/4%α-Si/2%void	+ 1106) 3893))- 4999	4686
617°C POLYSILICON DEPOSITION	87% Si 5% α-Si 8% void	4787	4350
+ DOPED & ANNEALED			

TABLE 3. Constituents and Film Thicknesses of Un-doped Annealed Wafers.

3A: POLYSILICON AS-DEPOSITED AT 580°C.

<u>BULKB14N</u>		<u>BULKB14O</u>	
(annealed in nitrogen)		(annealed in oxygen)	
99Å	SiO ₂	1066Å	SiO ₂
7Å	SiO	10Å	SiO
176Å	91% Si/9% α-Si	3109Å	90% Si/4% α-Si
3470Å	98% Si/2% α-Si	477Å	SiO ₂
468Å	SiO ₂	Substrate	Si
Substrate	Si		
<u>B14O</u>			
(BULKB14O with oxide overlayer removed)			
		10Å	SiO
		3096Å	98% Si/2% α-Si
		467Å	SiO ₂
		Substrate	Si

3B: POLYSILICON AS-DEPOSITED AT 617°C AND OXIDE OVERLAYER ETCHED-OFF.

<u>B20N</u>		<u>B20O</u>	
(annealed in nitrogen)		(annealed in oxygen)	
140Å	36% Si/36% α-Si/28% void	112Å	37% Si/36% α-Si/27% void
1062Å	72% Si/20% α-Si/8% void	1130Å	69% Si/24% α-Si/7% void
3686Å	91% Si/5% α-Si/4% void	2928Å	92% Si/5% α-Si/3% void
446Å	SiO ₂	574Å	SiO ₂
Substrate	Si	Substrate	Si

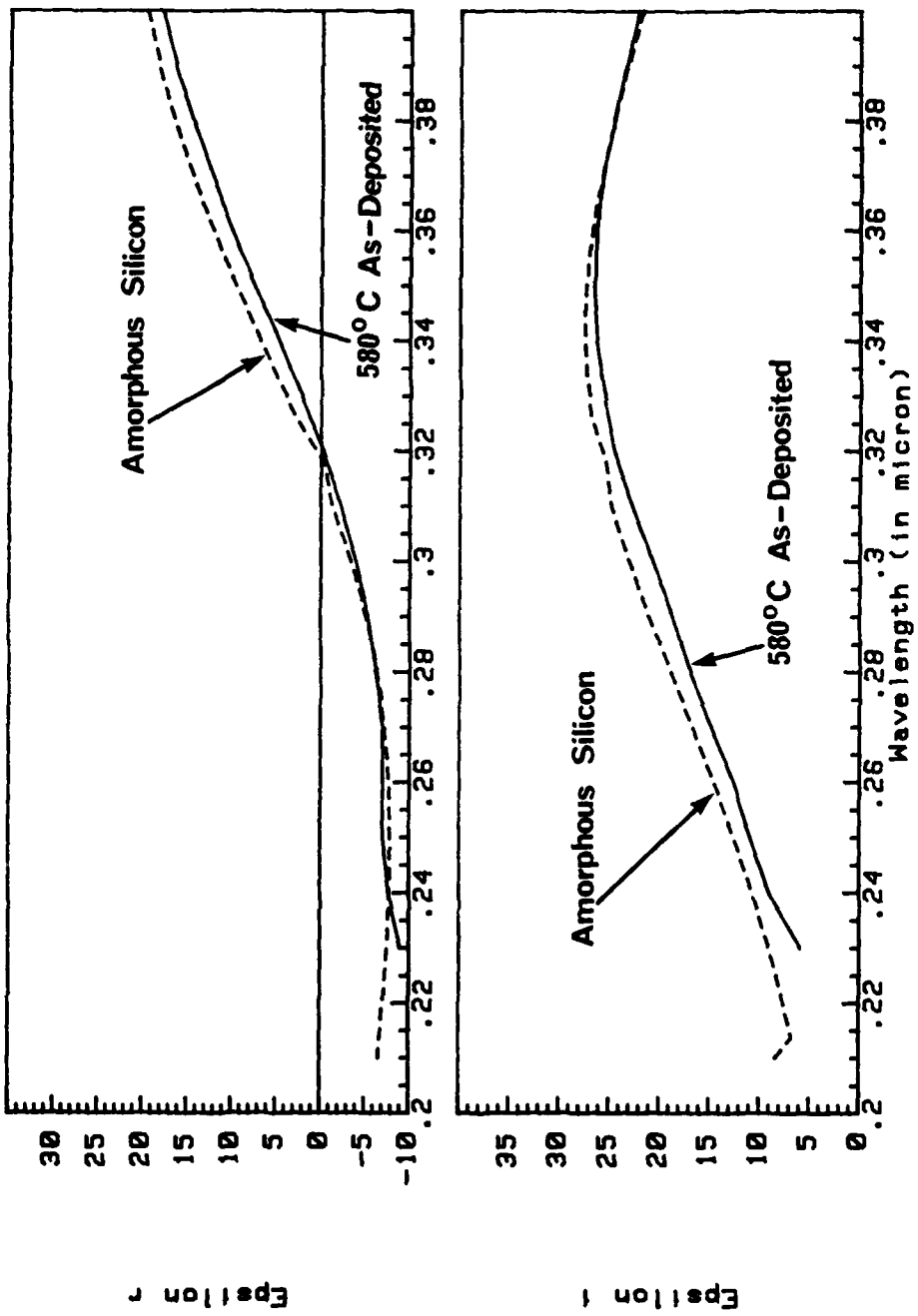


FIGURE 2 580°C AS-DEPOSITED & AMORPHOUS Si

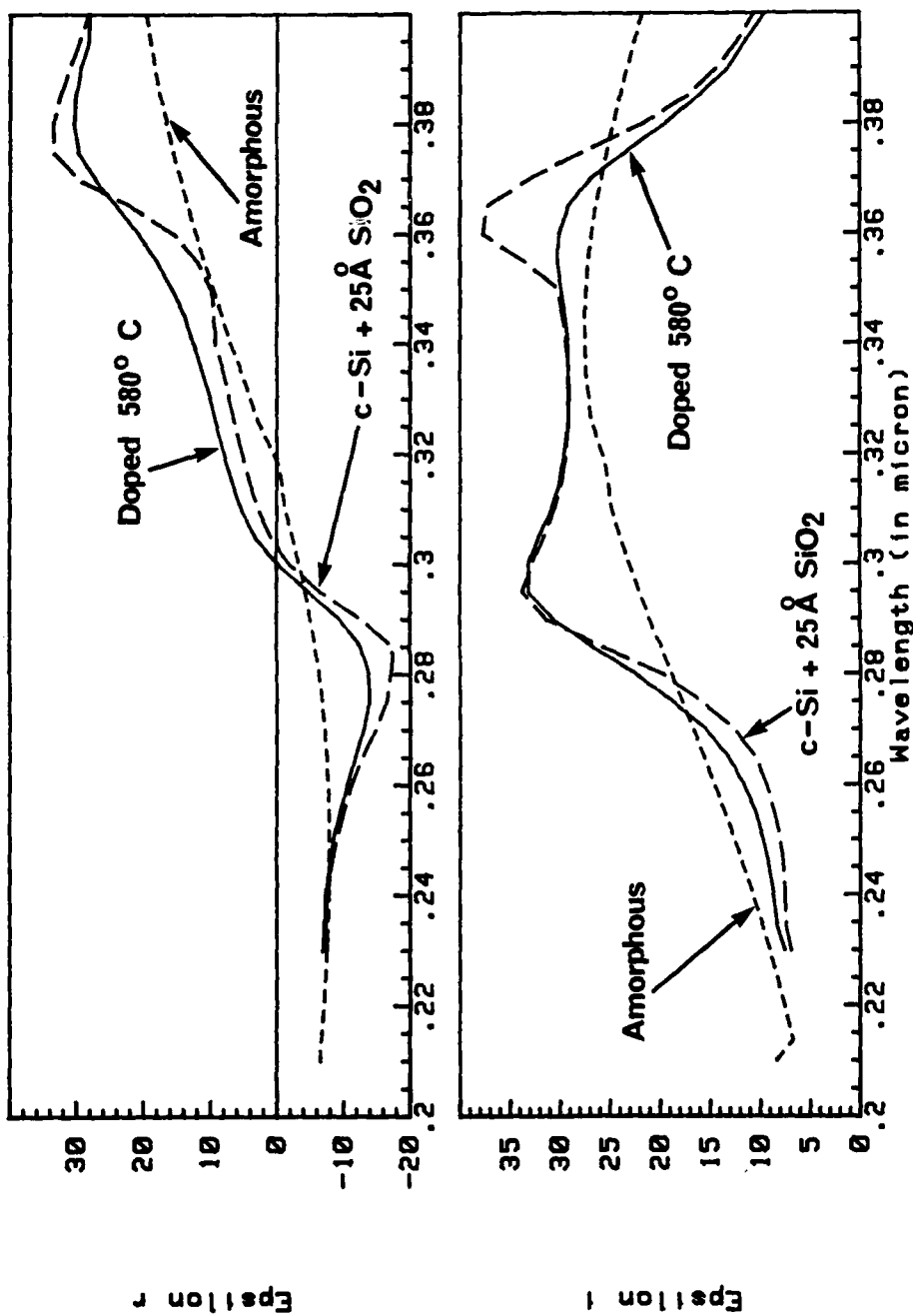


FIGURE 3b 580°C, DOPED 580°C & c-Si + 25 Å SiO₂

Fig. 3C. POLYSILICON ON OXIDISED BULK SILICON

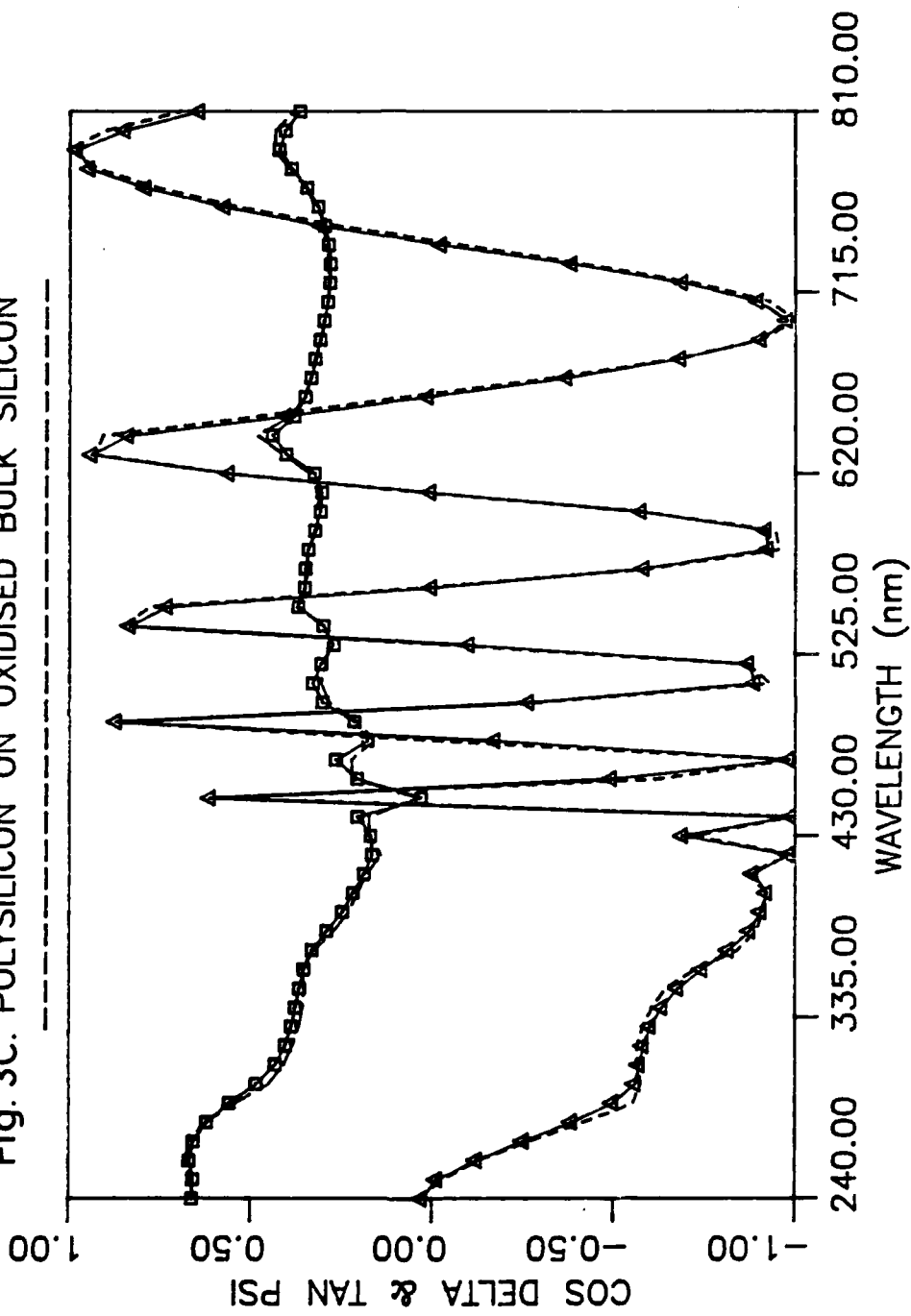
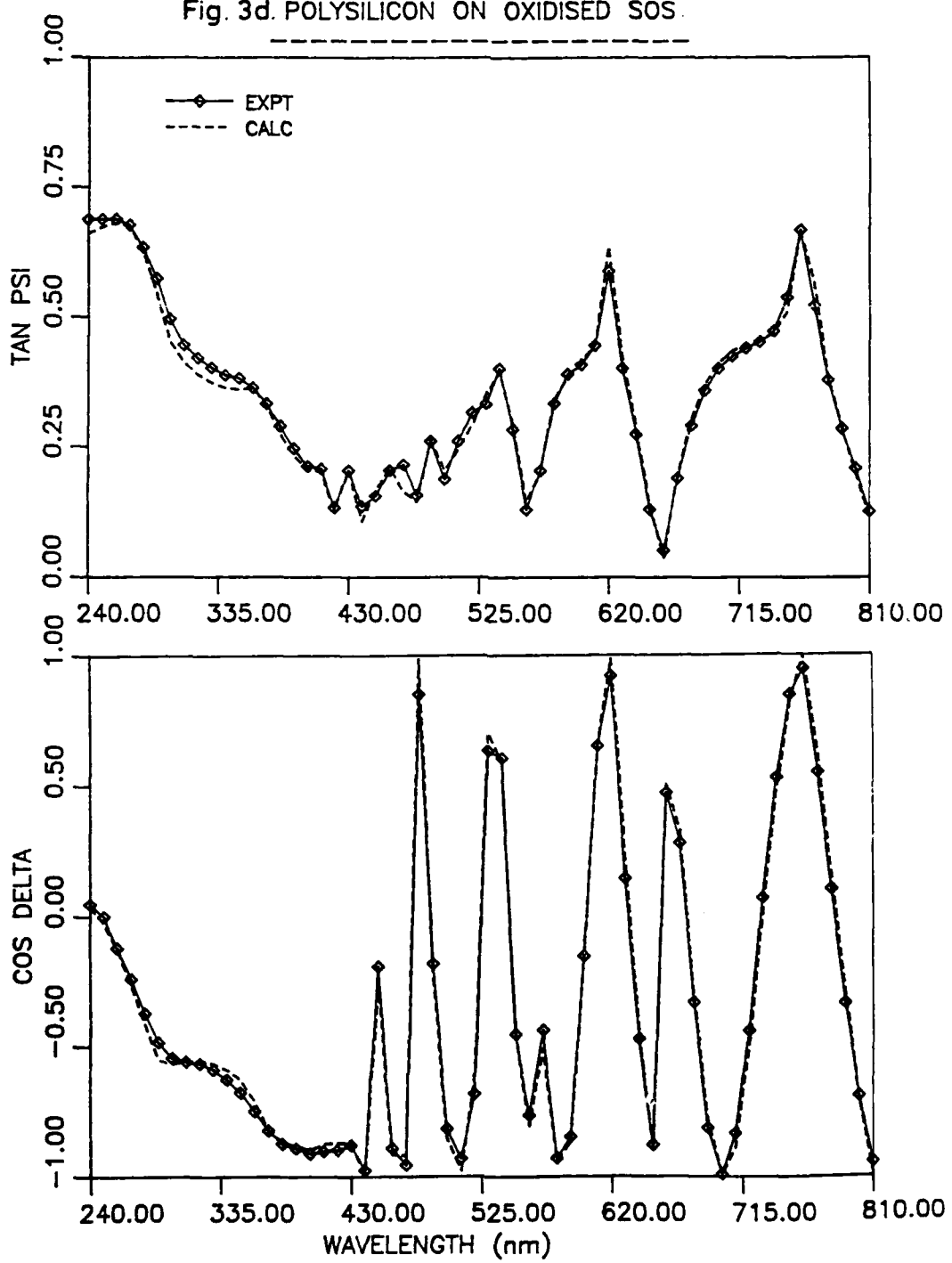


Fig. 3d. POLYSILICON ON OXIDISED SOS.



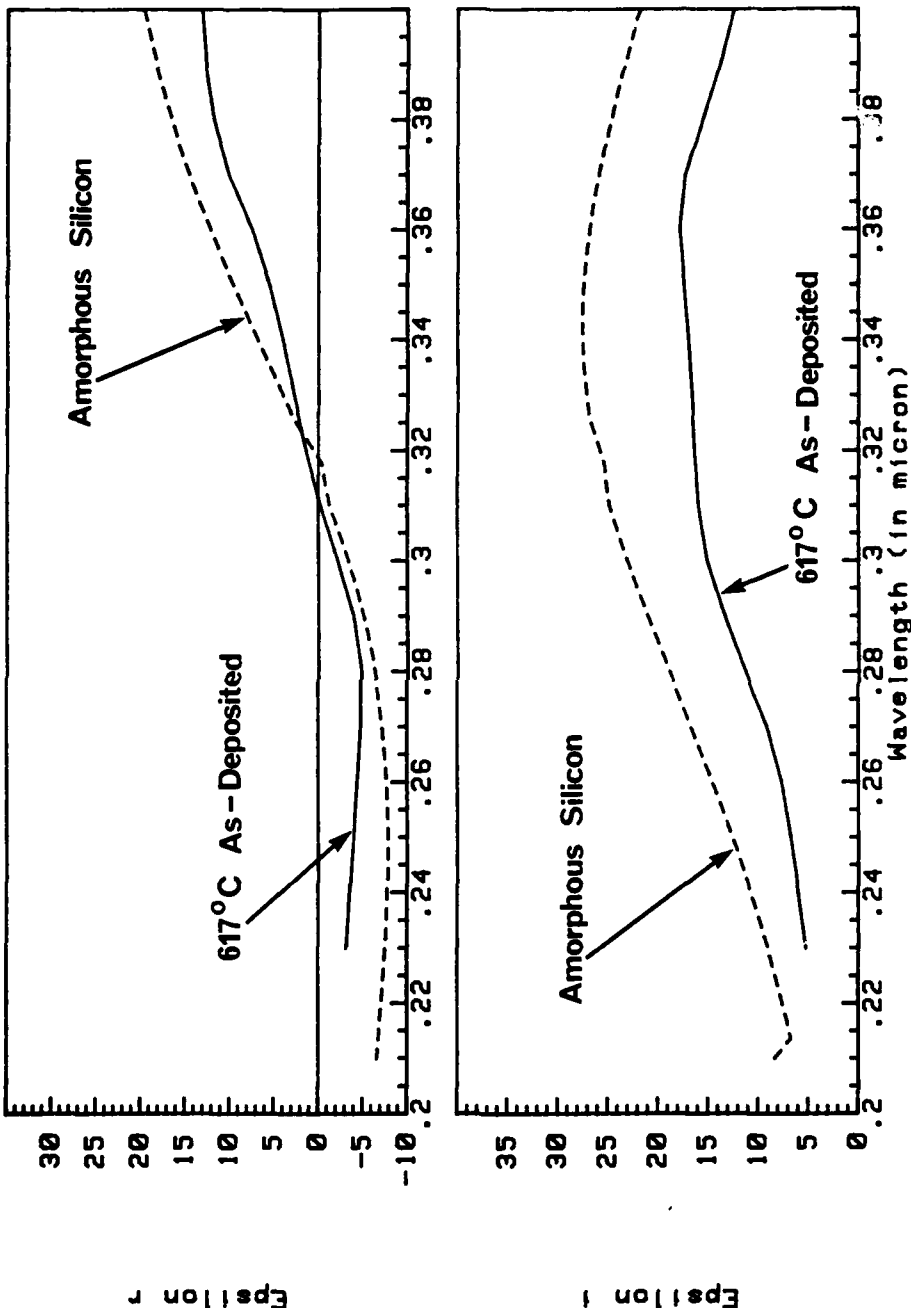


FIGURE 5 617°C AS - DEPOSITED & AMORPHOUS Si

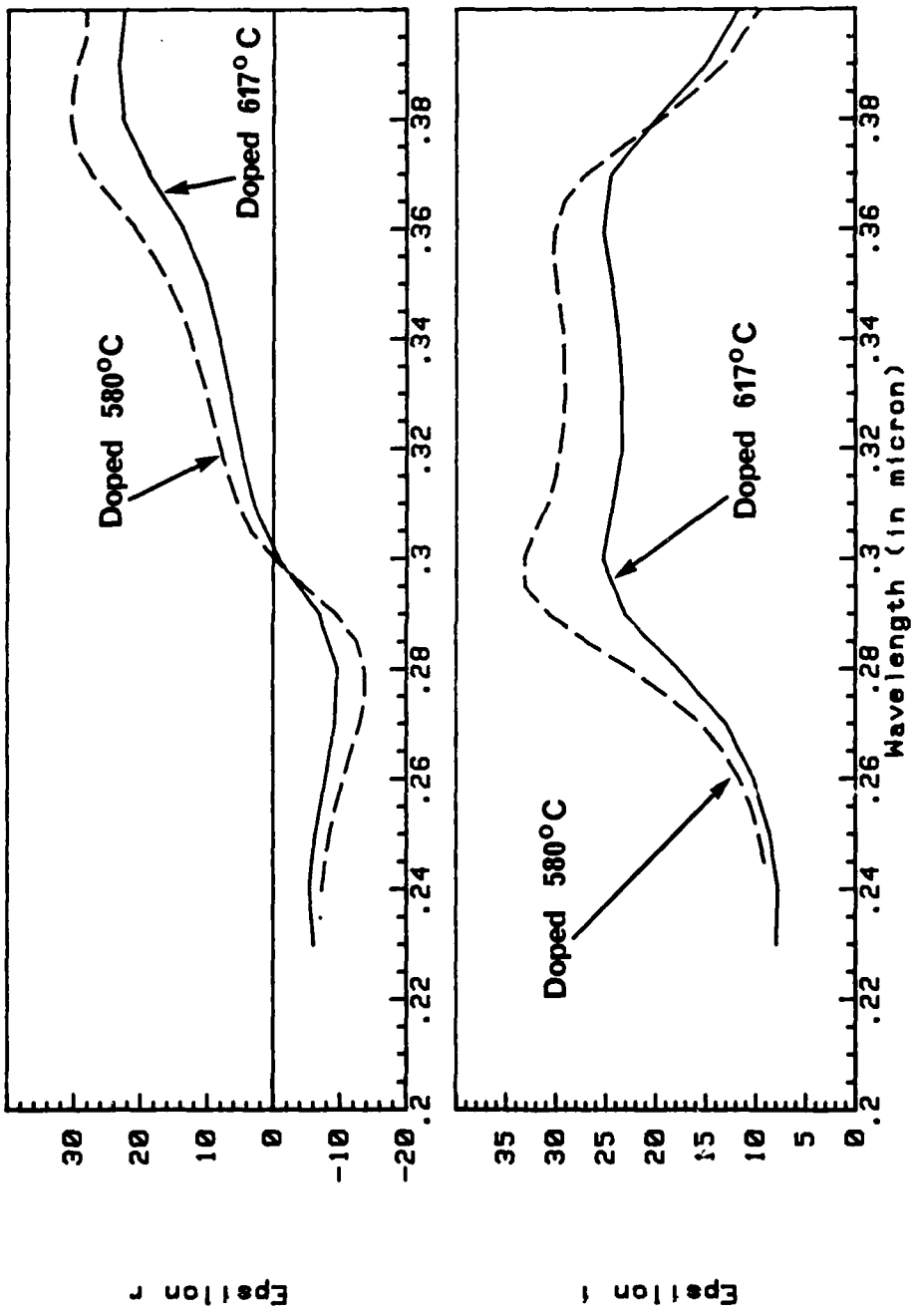


FIGURE 6b DOPED 580°C & DOPED 617°C SPECTRA

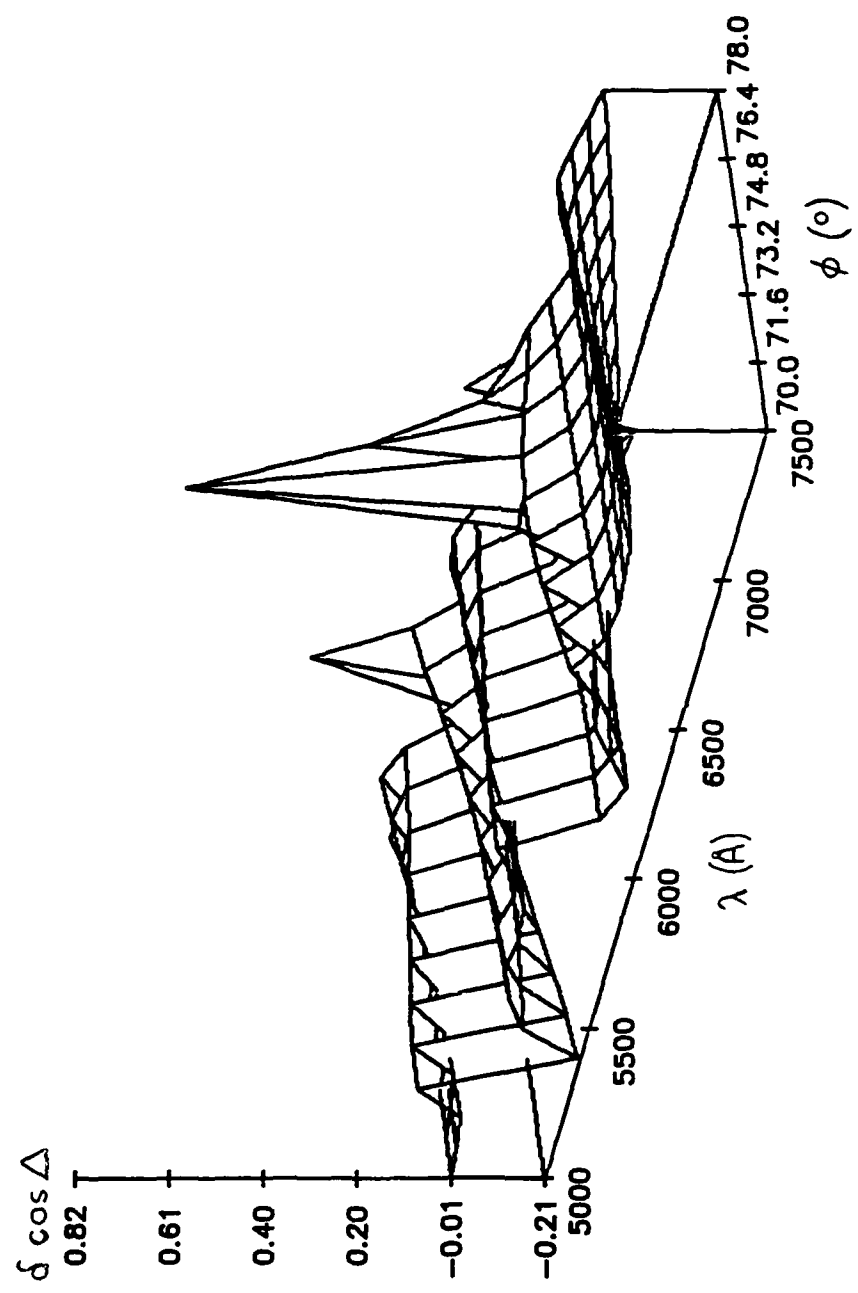


Figure 7a. Variance in $\cos \Delta$ (for a 50 Å change in buried SiO₂ layer thickness) VS Angle of incidence

Fig. 7b. Contour plot of $\cos \Delta$ peaks vs wavelength and angle of incidence

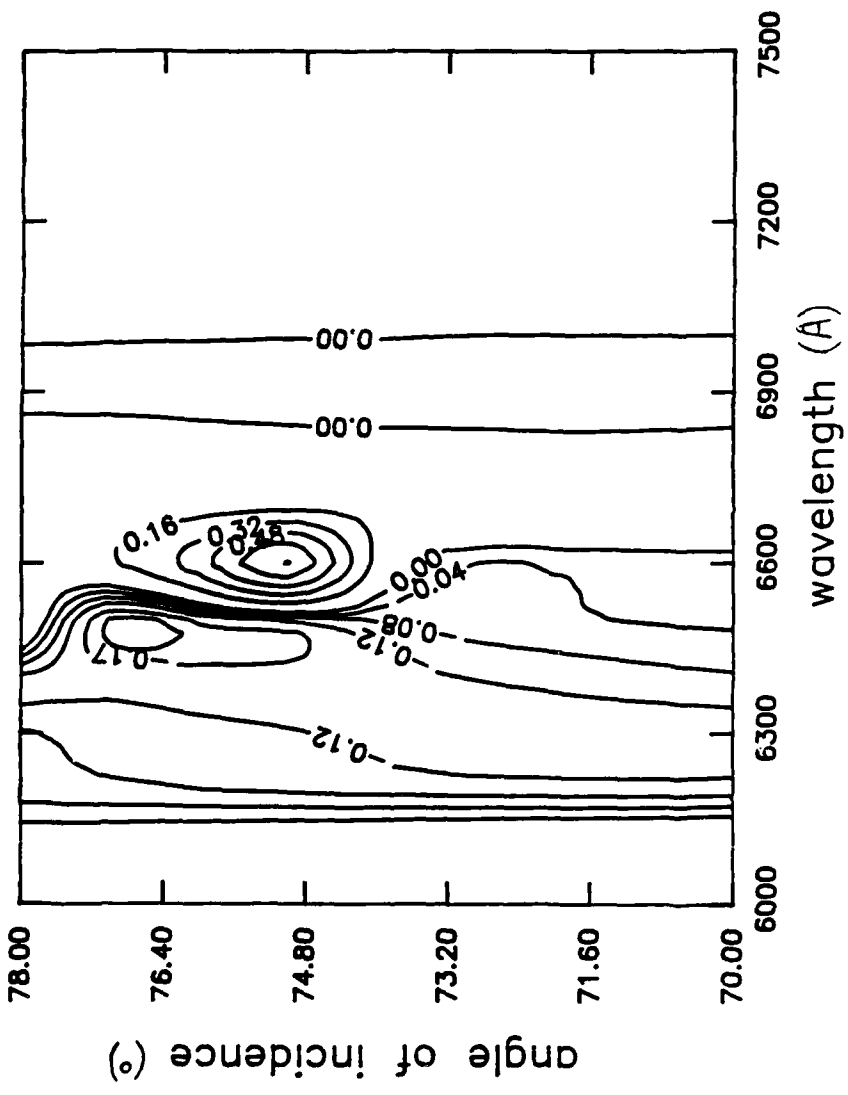
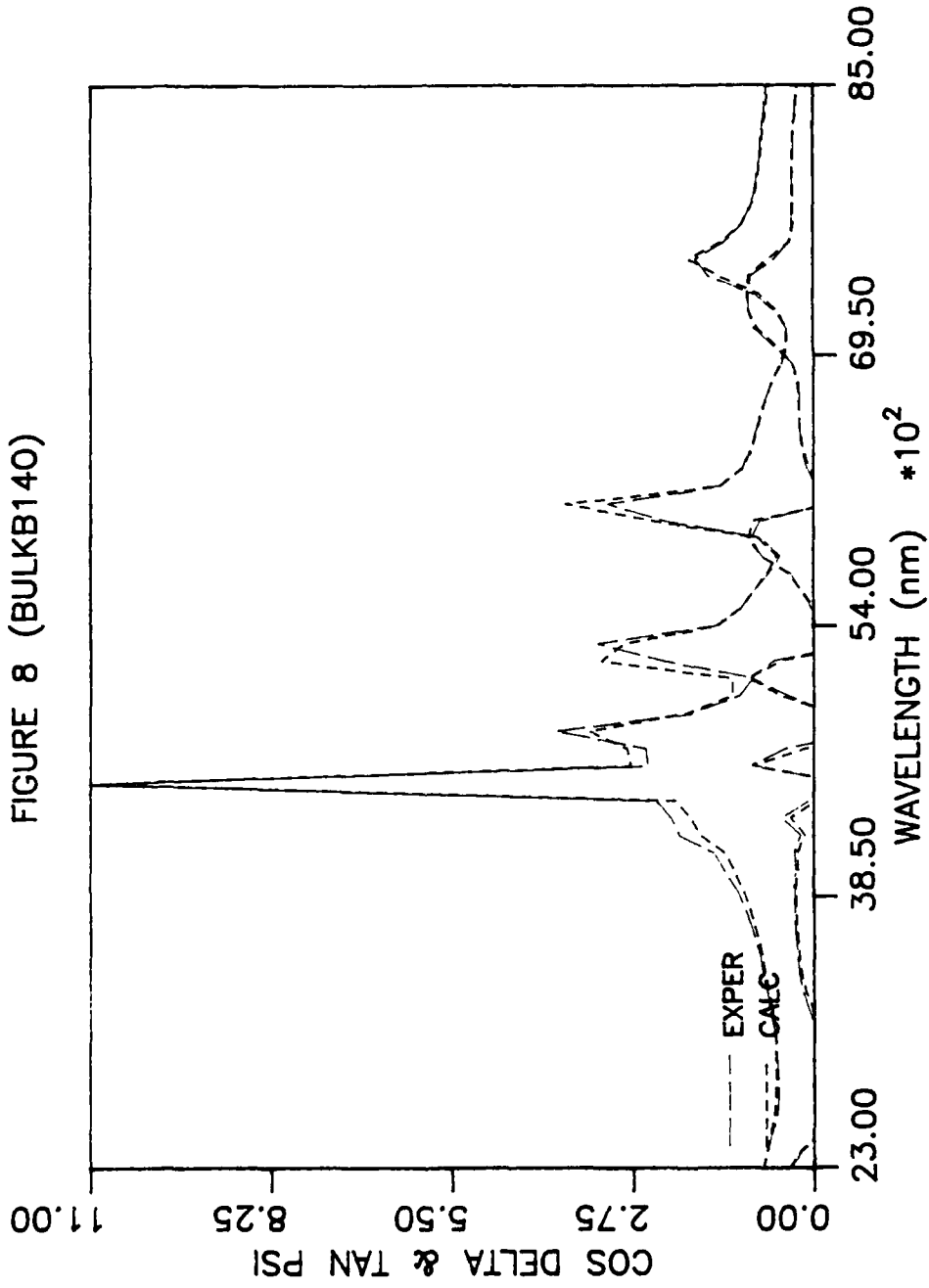


FIGURE 8 (BULKB140)



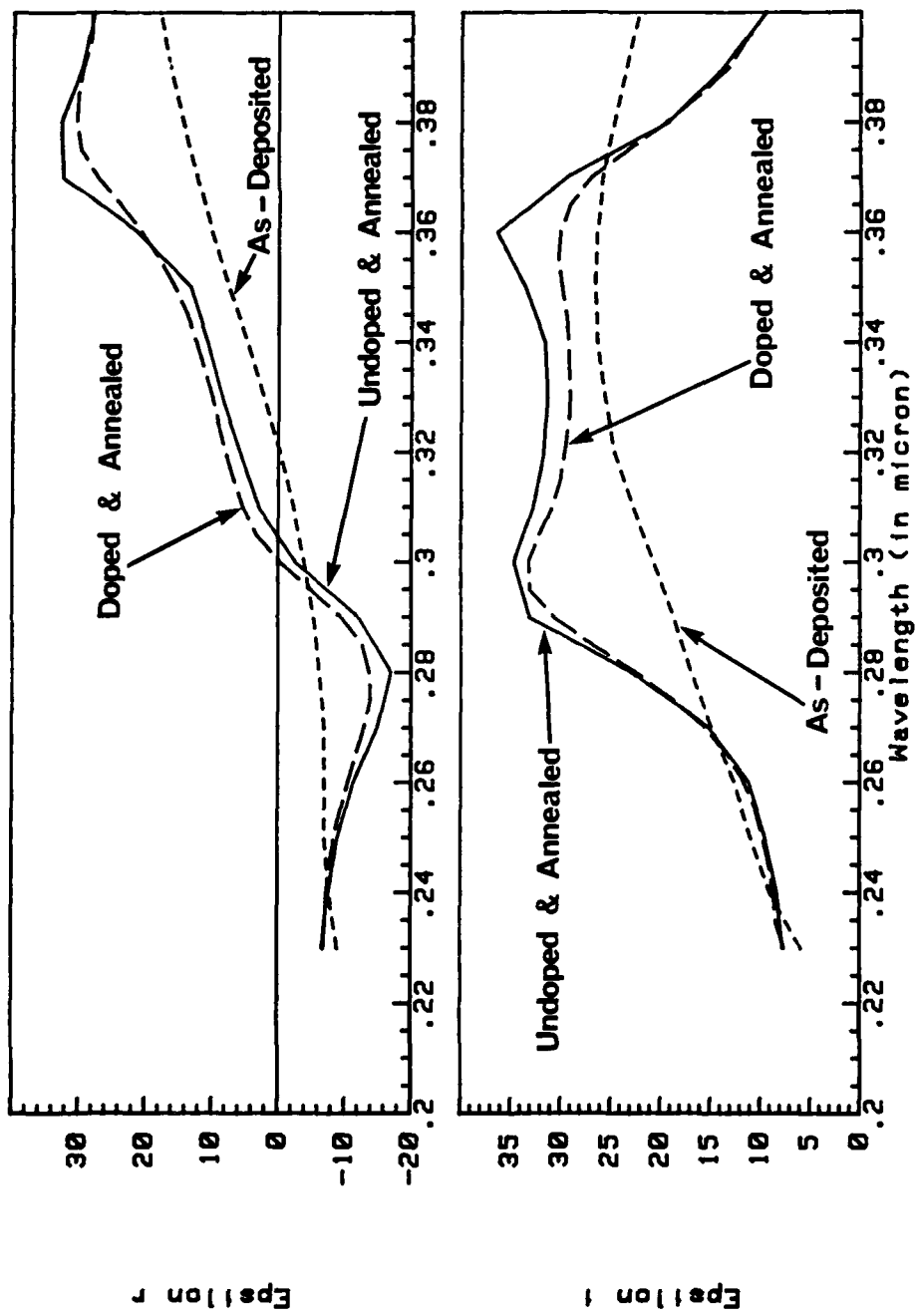


FIGURE 9 COMPARISON OF 580°C SAMPLES

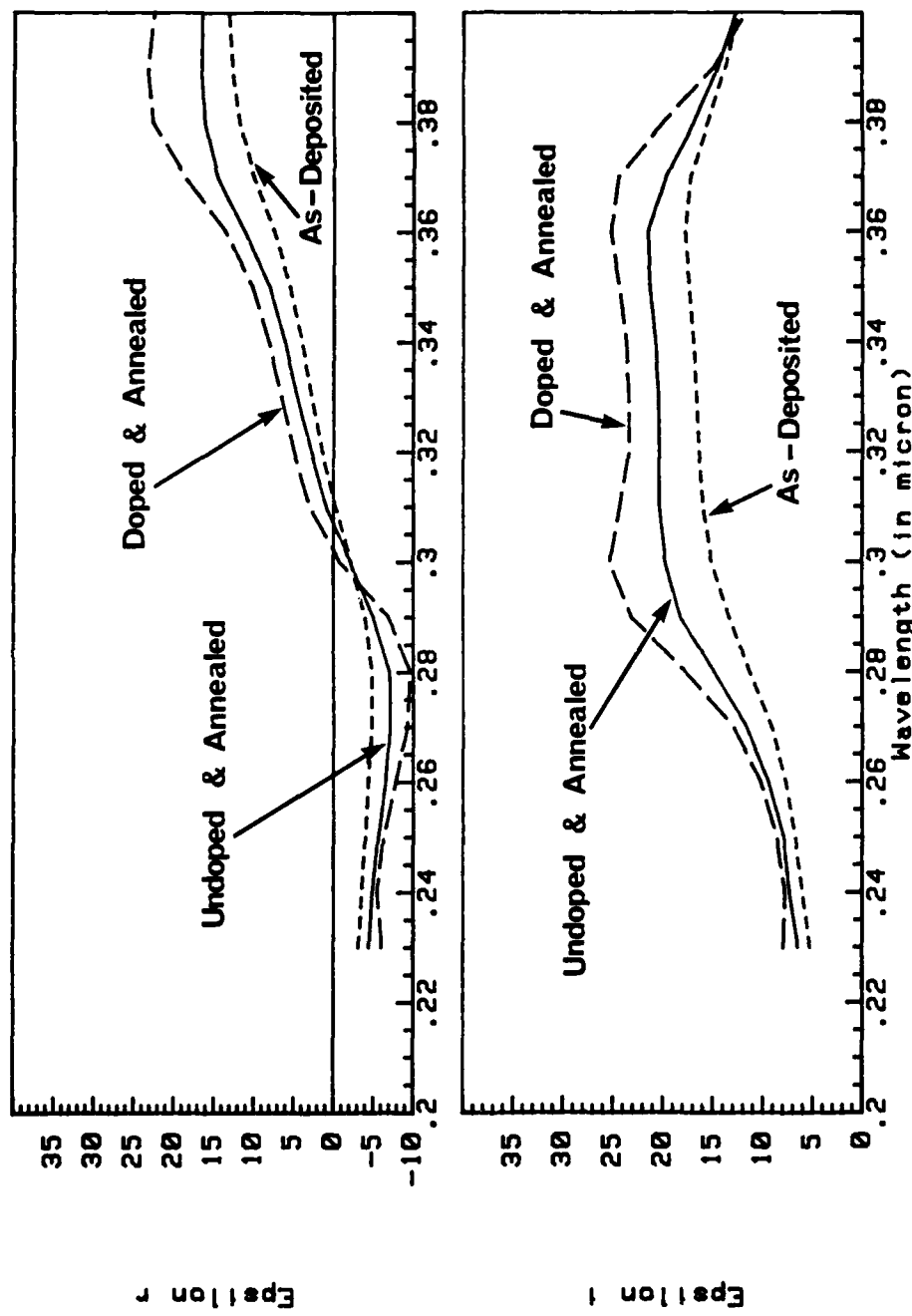


FIGURE 10 COMPARISON OF 617°C SAMPLES

DOCUMENT CONTROL SHEET

UNCLASSIFIED

Overall security classification of sheet

(As far as possible this sheet should contain only unclassified information. If it is necessary to enter classified information, the box concerned must be marked to indicate the classification eg (R) (C) or (S))

1. DRIC Reference (if known)	2. Originator's Reference Memo 4258	3. Agency Reference	4. Report Security Classification Unclassified	
5. Originator's Code (if known) 7784000	6. Originator (Corporate Author) Name and Location ROYAL SIGNALS & RADAR ESTABLISHMENT ST ANDREWS ROAD, GREAT MALVERN, WORCESTERSHIRE WR14 3PS			
5a. Sponsoring Agency's Code (if known)	6a. Sponsoring Agency (Contract Authority) Name and Location			
7. Title				
7a. Title in Foreign Language (in the case of translations) Spectroscopic ellipsometry characterisation of CVD deposition and doping of polysilicon multilayer structures				
7b. Presented at (for conference papers) Title, place and date of conference				
B. Author 1 Surname, initials Sharma S	9(a) Author 2 Pickering C	9(b) Authors 3,4... Morpeth A Terry G R	10. Date 10.1988	pp. ref. Up
11. Contract Number	12. Period	13. Project	14. Other Reference	
15. Distribution statement Unlimited				
Descriptors (or keywords)				
continue on separate piece of paper				
<p>Abstract</p> <p>Polysilicon multilayer structures were prepared by a CVD process. Spectroscopic ellipsometry supported by a computer modelling facility was used to synthesise models of the polysilicon-on-oxidised-silicon multilayer structures. Deposition temperature, recrystallisation and doping were studied on both bulk and SOS silicon wafers. The accuracy of interferometry as a film thickness measurement technique on polysilicon was also assessed.</p> <p style="text-align: right;">(J23)</p>				